

Static Analysis of Moderately Thick, Composite, Circular Rods via Mixed FEM

Ü.N. Arıbaş, A. Kutlu, and M.H. Omurtag

Abstract—The objective of this study is to investigate the static analysis of symmetrically and anti-symmetrically laminated elastic orthotropic composite circular rods with rectangular cross-section under the influence of distributed forces based on the mixed finite element method with Timoshenko theory. The Poisson's ratios are incorporated in the constitutive relation.

Index Terms— Circular rods, Composite Material, Mixed Finite Elements, Static Analysis

I. INTRODUCTION

THE increased use of composites in many applications such as aerospace, biomedical, mechanical, aircrafts, marine industry, robot arms, *etc.* due to their attractive properties in strength, stiffness and lightness has resulted in a growing demand for engineers in the design of laminated structures made of fiber-reinforced composite materials. Numerical texts dealing with the mechanics of composites by using various beam theories have been published to satisfy this demand [1]-[11]. Although the static analysis of laminated elastic isotropic and transversely isotropic composite rods is investigated intensively in the literature, studies with orthotropic lay-ups are quite rare.

In order to achieve maximum structural efficiency, designing laminates made of laminae that have different ply angles is a necessity. In this study, the Poisson's ratios are incorporated in the constitutive relations not to cause loss of some stiffness coefficients for angle-ply laminae. The constitutive equations of generally layered orthotropic rods are derived by reducing the constitutive relations of orthotropic materials for three-dimensional body [12]. Mixed finite element method with Timoshenko beam theory is used. The determination of the functional is based on the procedure given by [13] using Gâteaux differential [14].

II. CONSTITUTIVE RELATIONS OF COMPOSITE RODS

A. Constitutive Relations for a Single Lamina

The generalized Hooke's laws for elasticity and compliance matrices are defined as,

$$\boldsymbol{\sigma} = \mathbf{E} : \boldsymbol{\varepsilon} \quad \text{or} \quad \boldsymbol{\varepsilon} = \mathbf{C} : \boldsymbol{\sigma} \quad (1)$$

where, $\boldsymbol{\sigma}$, $\boldsymbol{\varepsilon}$, \mathbf{E} and \mathbf{C} ($=\mathbf{E}^{-1}$) denotes the stress tensor, strain tensor, elasticity matrix and compliance matrix, respectively. The constitutive relations of a transversely

orthotropic material have different material properties in three mutually perpendicular directions at a point of the body and further perpendicular planes of material property symmetry. Thus,

$$\begin{Bmatrix} \sigma_1 \\ \sigma_2 \\ \sigma_3 \\ \tau_{23} \\ \tau_{31} \\ \tau_{12} \end{Bmatrix} = \begin{bmatrix} E_{11} & E_{12} & E_{13} & 0 & 0 & 0 \\ E_{12} & E_{22} & E_{23} & 0 & 0 & 0 \\ E_{13} & E_{23} & E_{33} & 0 & 0 & 0 \\ 0 & 0 & 0 & E_{44} & 0 & 0 \\ 0 & 0 & 0 & 0 & E_{55} & 0 \\ 0 & 0 & 0 & 0 & 0 & E_{66} \end{bmatrix} \begin{Bmatrix} \varepsilon_1 \\ \varepsilon_2 \\ \varepsilon_3 \\ \gamma_{23} \\ \gamma_{31} \\ \gamma_{12} \end{Bmatrix} \quad (2)$$

Each layer in a laminate can have principal material direction orientations via versus to global laminate axes to meet the particular requirements of stiffness and strength. Thus, the transformation between the principle axes of the laminae and the global axes of the laminate must be considered.

$$\bar{\boldsymbol{\sigma}} = (\mathbf{T}^{-1} : \mathbf{E} : \mathbf{T}^{-T}) : \bar{\boldsymbol{\varepsilon}} = \bar{\mathbf{E}} : \bar{\boldsymbol{\varepsilon}} \quad (3)$$

where, \mathbf{T} is the transformation matrix.

$$\bar{\mathbf{E}} = \begin{bmatrix} \bar{E}_{11} & \bar{E}_{12} & \bar{E}_{13} & 0 & 0 & \bar{E}_{16} \\ \bar{E}_{12} & \bar{E}_{22} & \bar{E}_{23} & 0 & 0 & \bar{E}_{26} \\ \bar{E}_{13} & \bar{E}_{23} & \bar{E}_{33} & 0 & 0 & \bar{E}_{36} \\ 0 & 0 & 0 & \bar{E}_{44} & \bar{E}_{45} & 0 \\ 0 & 0 & 0 & \bar{E}_{45} & \bar{E}_{55} & 0 \\ \bar{E}_{16} & \bar{E}_{26} & \bar{E}_{36} & 0 & 0 & \bar{E}_{66} \end{bmatrix} \quad (4)$$

More detailed information about the components of elasticity matrices in Eqns. (2) and (4), and the transformation matrix for a rotation about b-axis (Fig 1.) exists in [15].

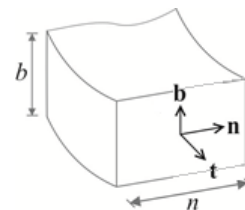


Fig. 1. Frenet coordinates of the circular rod with a rectangular cross-section.

The constitutive equations for a single lamina are derived by reducing the constitutive equations of orthotropic materials for three-dimensional body. The assumptions made on stresses, in accordance with the classical rod theory, are as follows [16],

$$\sigma_n = \sigma_b = \tau_{nb} = 0 \quad (5)$$

where, the stress components in Frenet coordinates via versus in a three dimensional body are,

Manuscript received March 02, 2016; revised April 06, 2016.
All authors are with Istanbul Technical University, 34469, Istanbul, TURKEY
Email of the corresponding author : umitaribas@hotmail.com

$$\begin{aligned} \sigma_t &= \sigma_1, & \sigma_n &= \sigma_2, & \sigma_b &= \sigma_3 \\ \tau_{nb} &= \tau_{23}, & \tau_{bt} &= \tau_{31}, & \tau_m &= \tau_{12} \end{aligned} \quad (6)$$

By paying attention to Eqns. (1), (4) and (5), the strain components $\epsilon_b, \epsilon_n, \gamma_{nb}$ are calculated with respect to the ϵ_t, γ_{bt} and γ_m for the rods and inserted into the equalities [12],

$$\begin{Bmatrix} \sigma_t \\ \tau_{bt} \\ \tau_m \end{Bmatrix} = \begin{bmatrix} \beta_{11} & 0 & \beta_{13} \\ 0 & \beta_{22} & 0 \\ \beta_{13} & 0 & \beta_{33} \end{bmatrix} \begin{Bmatrix} \epsilon_t \\ \gamma_{bt} \\ \gamma_m \end{Bmatrix} \quad (7)$$

The displacements of an arbitrary point on the cross-section for a circular rod (Fig. 1) are stated as,

$$\begin{aligned} u_t^* &= u_t + b \Omega_n - n \Omega_b \\ u_n^* &= u_n - b \Omega_t \\ u_b^* &= u_b + n \Omega_t \end{aligned} \quad (8)$$

where, u_t^*, u_n^*, u_b^* are displacements at the rod continuum and u_t, u_n, u_b are displacements on the rod axis and Ω_t, Ω_n and Ω_b present the rotations of the rod on the t, n and b Frenet Coordinates, respectively. The strains can be derived from Eqn. (8) as [17],

$$\begin{Bmatrix} \epsilon_t \\ \gamma_{bt} \\ \gamma_m \end{Bmatrix} = \begin{Bmatrix} \frac{\partial u_t}{\partial t} \\ \frac{\partial u_t}{\partial b} + \frac{\partial u_b}{\partial t} \\ \frac{\partial u_t}{\partial n} + \frac{\partial u_n}{\partial t} \end{Bmatrix} + b \begin{Bmatrix} \frac{\partial \Omega_n}{\partial t} \\ 0 \\ \frac{\partial \Omega_t}{\partial t} \end{Bmatrix} + n \begin{Bmatrix} -\frac{\partial \Omega_b}{\partial t} \\ \frac{\partial \Omega_t}{\partial t} \\ 0 \end{Bmatrix} \quad (9)$$

B. Lamination

A lamina is a flat arrangement of the laminate. When a stack of laminae with various orientations of principle material directions are bonded together and act as an integral structural element to match the loading environment by tailoring the directional dependence of strength and stiffness of the structural element and get corrosion resistance, acoustical insulation and temperature-dependent behavior, etc. is called laminate. It is assumed that the strain distribution is linear through the laminate thickness and no slip occurs between the boundaries of laminae but the stress distribution has discontinuities at boundaries between laminae. Thus, the forces and moments for a laminate can be derived by analytical integration of the stresses in each lamina through the thickness of the laminate.

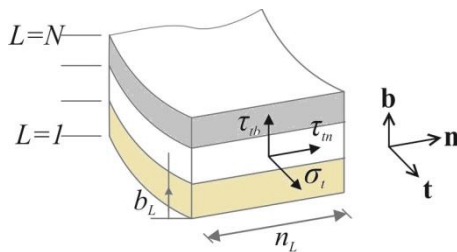


Fig. 2. The stresses with respect to the Frenet Coordinates, N: total number of layers.

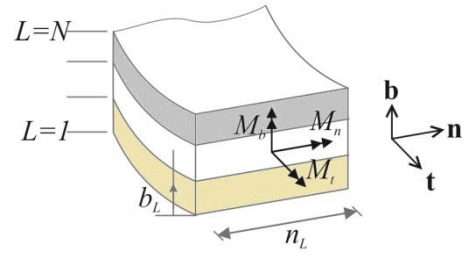


Fig. 3. The moments with respect to the Frenet Coordinates.

Namely; Derivation of forces,

$$T_t = \sum_{L=1}^N \left(\int_{-0.5n_L}^{0.5n_L} \left(\int_{b_{L-1}}^{b_L} \sigma_t db \right) dn \right) \quad (10)$$

$$T_b = \sum_{L=1}^N \left(\int_{-0.5n_L}^{0.5n_L} \left(\int_{b_{L-1}}^{b_L} \tau_{bt} db \right) dn \right) \quad (11)$$

$$T_n = \sum_{L=1}^N \left(\int_{-0.5n_L}^{0.5n_L} \left(\int_{b_{L-1}}^{b_L} \tau_m db \right) dn \right) \quad (12)$$

Derivation of moments,

$$\begin{aligned} M_t &= \sum_{L=1}^N \left(- \int_{-0.5n_L}^{0.5n_L} \left(\int_{b_{L-1}}^{b_L} b \tau_m db \right) dn \right) \\ &+ \sum_{L=1}^N \left(\int_{b_{L-1}}^{b_L} \left(\int_{-0.5n_L}^{0.5n_L} n \tau_{bt} dn \right) db \right) \end{aligned} \quad (13)$$

$$M_n = \sum_{L=1}^N \left(\int_{-0.5n_L}^{0.5n_L} \left(\int_{b_{L-1}}^{b_L} b \sigma_t db \right) dn \right) \quad (14)$$

$$M_b = - \sum_{L=1}^N \left(\int_{b_{L-1}}^{b_L} \left(\int_{-0.5n_L}^{0.5n_L} n \sigma_t dn \right) db \right) \quad (15)$$

where, N is the number of the laminae in a laminate, n_L is the width of the layer and b_L and b_{L-1} are the directed distances to the bottom and the top of the L^{th} layer where b is positive upward. Finally, the constitutive relations are obtained by using Eqns. (10)-(15) in a matrix form:

$$\begin{Bmatrix} T_t \\ T_n \\ T_b \\ M_t \\ M_n \\ M_b \end{Bmatrix} = \sum_{L=1}^N \begin{bmatrix} \mathbf{E}_T^L & \mathbf{E}_{TM}^L \\ \mathbf{E}_{MT}^L & \mathbf{E}_M^L \end{bmatrix} \begin{Bmatrix} \frac{\partial u_t}{\partial t} \\ \frac{\partial u_t}{\partial n} + \frac{\partial u_n}{\partial t} \\ \frac{\partial u_t}{\partial b} + \frac{\partial u_b}{\partial t} \\ \frac{\partial \Omega_t}{\partial t} \\ \frac{\partial \Omega_n}{\partial t} \\ \frac{\partial \Omega_b}{\partial t} \end{Bmatrix} \quad (16)$$

\mathbf{E}_{TM}^L and \mathbf{E}_{MT}^L are coupling matrices. Also please note that $\mathbf{E}_{TM}^L = (\mathbf{E}_{MT}^L)^T$. The compliance matrix of a laminate is obtained by $\mathbf{C} = \mathbf{E}^{-1}$.

C. Functional

The field equations based on Timoshenko beam theory for a curved rod can be given as [18].

Equilibrium Equations;

$$\begin{aligned} -\frac{d\mathbf{T}}{ds} - \mathbf{q} + \rho A \ddot{\mathbf{u}} &= 0 \\ -\frac{d\mathbf{M}}{ds} - \mathbf{t} \times \mathbf{T} - \mathbf{m} + \rho \mathbf{I} \ddot{\boldsymbol{\Omega}} &= 0 \end{aligned} \quad (17)$$

Kinematic Equations;

$$\begin{aligned} -\mathbf{C}_{MT} \mathbf{T} - \mathbf{C}_M \mathbf{M} + \frac{d\boldsymbol{\Omega}}{ds} &= 0 \\ -\mathbf{C}_T \mathbf{T} - \mathbf{C}_{TM} \mathbf{M} + \frac{d\mathbf{u}}{ds} + \mathbf{t} \times \boldsymbol{\Omega} &= 0 \end{aligned} \quad (18)$$

In general sense, the field equations can be written in an operator form $\mathbf{Q} = \mathbf{L}\bar{\mathbf{y}} - \bar{\mathbf{f}}$ and if the operator is potential, the equality $\langle d\mathbf{Q}(\bar{\mathbf{y}}, \tilde{\bar{\mathbf{y}}}), \bar{\mathbf{y}}^* \rangle = \langle d\mathbf{Q}(\bar{\mathbf{y}}, \bar{\mathbf{y}}^*), \tilde{\bar{\mathbf{y}}} \rangle$ must be satisfied [18]. $d\mathbf{Q}(\bar{\mathbf{y}}, \tilde{\bar{\mathbf{y}}})$ and $d\mathbf{Q}(\bar{\mathbf{y}}, \bar{\mathbf{y}}^*)$ are Gâteaux derivatives of the operator in directions of $\tilde{\bar{\mathbf{y}}}$ and $\bar{\mathbf{y}}^*$. After proving the operator to be potential, the functional including the rotary inertia and shear influence is obtained as follows:

$$\begin{aligned} I(\mathbf{y}) = & -\left[\frac{d\mathbf{T}}{ds}, \mathbf{u} \right] - \left[\frac{d\mathbf{M}}{ds}, \boldsymbol{\Omega} \right] - [\mathbf{q}, \mathbf{u}] - [\mathbf{m}, \boldsymbol{\Omega}] \\ & + [\mathbf{t} \times \boldsymbol{\Omega}, \mathbf{T}] - \frac{1}{2} \{ [\mathbf{C}_T \mathbf{T}, \mathbf{T}] + [\mathbf{C}_{TM} \mathbf{M}, \mathbf{T}] \\ & + [\mathbf{C}_{MT} \mathbf{T}, \mathbf{M}] + [\mathbf{C}_M \mathbf{M}, \mathbf{M}] \} + [\mathbf{T}, \hat{\mathbf{u}}]_{\epsilon} \\ & + [\mathbf{M}, \hat{\boldsymbol{\Omega}}]_{\epsilon} + [(\mathbf{T} - \hat{\mathbf{T}}), \mathbf{u}]_{\sigma} + [(\mathbf{M} - \hat{\mathbf{M}}), \boldsymbol{\Omega}]_{\sigma} \end{aligned} \quad (19)$$

where, \mathbf{q} is distributed external forces, \mathbf{m} is distributed external moments along the rod axis, \mathbf{C}_{TM} and \mathbf{C}_{MT} are coupling compliance matrices, \mathbf{u} are displacements on the rod axis, $\boldsymbol{\Omega}$ are rotations of the rod, \mathbf{T} are forces and \mathbf{M} are moments of cross-section and quantities with hat are known values on the boundary.

D. The Mixed Finite Element Algorithm

The linear shape functions $\phi_i = (\varphi_j - \varphi) / \Delta\varphi$ and $\phi_j = (\varphi - \varphi_i) / \Delta\varphi$ are employed in the finite element formulation, where $\Delta\varphi = (\varphi_j - \varphi_i)$. i, j represent the node numbers of the curved element. The field variables at a node are,

$$\mathbf{X}^T = \{u_i, u_n, u_b, \Omega_i, \Omega_n, \Omega_b, T_i, T_n, T_b, M_i, M_n, M_b\} \quad (20)$$

The curvatures are satisfied exactly at the nodal points and linearly interpolated through the element [19].

III. NUMERICAL EXAMPLES

Numerical results are verified by ANSYS 14.5 for the static analysis of a straight rod with three orthotropic lay-ups. Static analysis of symmetrically and anti-symmetrically layered cross-ply circular rod with four orthotropic lay-ups is investigated for three different lay-up conditions as benchmark example.

Orthotropic material properties used for convergence and benchmark examples are given as [16] in Table I.

TABLE I
MATERIAL PROPERTIES OF ORTHOTROPIC MATERIAL

Young's Modulus (N/m^2) $\times 10^9$	Shear Modulus (N/m^2) $\times 10^9$	Poisson's Ratio
$E_t = 39.3$	$G_m = 29.3$	$\nu_m = 0.613$
$E_n = 152$	$G_{tb} = 1.6$	$\nu_{tb} = 0.265$
$E_b = 22.9$	$G_{nb} = 4.1$	$\nu_{nb} = 0.209$

A. Convergence Analysis

Static analysis of symmetrically laminated elastic straight beam with three orthotropic cross-ply layers under the influence of distributed force is investigated. Both ends of the beam have fixed supports and 10 N/m distributed load applied along the length of the beam (18m). Each layer has the same orthotropic material properties given in Table I with different orientations ($0^\circ, 90^\circ, 0^\circ$). Dimensions of the thickness and width of layers are given in Figure 4.

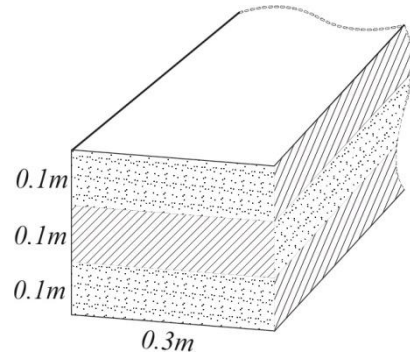


Fig. 4. Cross-section of the convergence example.

Results are obtained by ANSYS 14.5 with three bend solid layer elements fixed at supports, distributed load is applied at the top surface of top layer, core layer's orientation is given by applying a local Cartesian Coordinate system for core layer. A convergence analysis is performed for 20, 40, 60, 80 and 100 elements by using this study in order to attain the necessary precision for the results (Table II).

TABLE II
CONVERGENCE VIA VERSUS ANSYS

	MAX. DISP. (m) $\times 10^{-5}$	REACTION	
		FORCE (N)	MOMENT (Nm)
20	9.662	90	267.03
40	9.569	90	269.33
60	9.552	90	269.70
80	9.546	90	269.83
100	9.543	90	269.89
ANSYS	9.448	90	270.14

It is observed that the result are quite satisfactory, the reaction forces present better convergence than displacements. The maximum difference is obtained 1% for 60 elements compare to ANSYS solid elements.

B. Benchmark Examples

Static analysis of symmetrically and anti-symmetrically laminated elastic circular rod with four orthotropic cross-ply layers under the influence of distributed load are investigated. Both ends of the rod have fixed support, rod geometry is a half circle with 18m radius and 1 N/m out of plane distributed load applied along the length of the beam (Fig. 5).

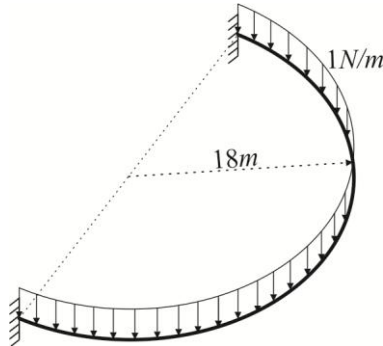


Fig. 5. Geometry of the rod for benchmark examples.

Each layer has the same orthotropic material properties given in Table I with different orientations (0°,90°,90°,0°), (90°,0°,0°,90°) and (0°,90°,0°,90°). Dimensions of the thickness and width of layers are given in Figure 6.

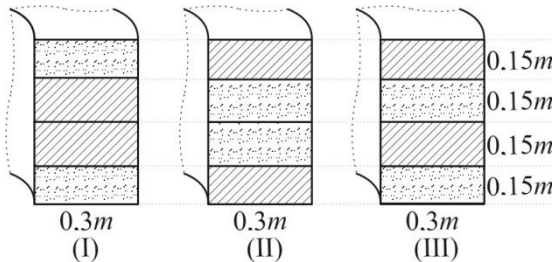


Fig. 6. Cross-section of benchmark examples.

Results given in Table III are obtained by using 40 finite elements for symmetric lamination, second and third layers are oriented 90° about b axis (I), top and bottom layers are oriented 90° about b axis (II) and anti-symmetric lamination, second and top layers are oriented 90° about b axis (III).

TABLE III
SYMMETRY AND ANTI-SYMMETRY CONDITION

	(I)	(II)	(III)	
REACTION	Max. Disp. (m) × 10 ⁻⁵	34.12	31.40	33.05
	Force (N)	28.27	28.27	28.27
	M _t (Nm)	95.30	95.01	95.10
	M _n (Nm)	325.56	326.06	325.90

It is observed from Table III, layer-wise material placement has great importance to reduce the maximum displacements while considering orthotropic layered laminated rods. Minimum displacement is obtained for symmetric condition (II), but anti-symmetric condition (III) presents lesser displacements compare to symmetric condition (II).

IV. CONCLUSION

In this study, the static analysis of symmetrically and anti-symmetrically laminated orthotropic circular rods under the influence of distributed forces are investigated. Convergence analysis of laminated straight rods made of orthotropic material have been done for various finite elements and the result are compared with ANSYS 14.5 due to the studies with orthotropic lay-ups are quite rare in the literature. Satisfactory results are obtained for constitutive equations of this study with 60 finite elements. As a benchmark example, symmetry condition is investigated for a circular rod with four orthotropic layers. It is observed that, in composite materials, layer-wise material placement along the thickness direction has great importance on the response the structure.

REFERENCES

- [1] I. K. Silverman, "Flexure of Laminated Beams", *Journal of the Structural Division*, vol. 106, no. 3, pp. 711-725, 1980.
- [2] M. Z. Hu, H. Kolsky and A. C. Pipkin, "Bending Theory for Fiber-reinforced Beams", *J. Composite Mater.*, vol. 19, pp. 235-249, 1985.
- [3] O. O. Ochoa and T. J. Kozik, "Transverse and Normal Stresses in Laminated Beams", *In Design and Analysis of Composite Material Vessels*, vol. 121, no. 11, pp. 1-8, 1987.
- [4] F. Gordaninejad and A. Ghazavi, "Bending of Thick Laminated Composite Beams Using a Higher-order Shear-deformable Beam Theory", *In design and Analysis of Composite Material Vessels*, vol. 121, no. 11, pp. 9-14, 1987.
- [5] R. K. Kapania and S. Raciti, "Recent Advances in Analysis of Laminated Beams and Plates, Part I: Shear Effects and Buckling", *AIAA Journal*, vol. 27, no. 7, pp. 923-935, 1989.
- [6] A. A. Khdeir and J. N. Reddy, "An Exact Solution for the Bending of Thin and Thick Cross-ply Laminated Beams", *Composite Structures*, vol. 37, pp. 195-203, 1997.
- [7] S. R. Swanson, "Torsion of Laminated Rectangular Rods", *Composite Structures*, vol. 42, pp. 23-31, 1998.
- [8] G. J. Kennedy, J. S. Hansen and R. R. A. Martins, "A Timoshenko Beam Theory with Pressure Corrections for Layered Orthotropic Beams", *International Journal of Solids and Structures*, vol. 48, pp. 2373-2382, 2011.
- [9] R. M. Aguiar, F. Moleiro and C. M. Mota Soares, "Assessment of Mixed and Displacement-based Models for Static Analysis of Composite Beams of Different Cross-sections", *Composite Structures*, vol. 94, no. 2, pp. 601-616, 2012.
- [10] T. P. Vo and HT. Thai, "Static Behavior of Composite Beams Using Various Refined Shear Deformation Theories", *Composite Structures*, vol. 94, no. 8, pp. 2513-2522, 2012.
- [11] S. Nagarajan and A. R. Zak, "Finite Element Model for Orthotropic Beams", *Composite Materials and Structures*, vol. 20, no. 1-3, pp. 443-449, 1985.
- [12] A. Bhimaraddi and K. Chandrashekhara, "Some Observations on The Modelling of Laminated Composite Beams with General Lay-ups", *Composite Structures*, vol. 19, pp. 371-380, 1991.
- [13] M. H. Omurtag and A. Y. Aköz, "The Mixed Finite Element Solution of Helical Beams with Variable Cross-Section Under Arbitrary Loading", *Computers and Structures*, vol. 43, pp. 325-331, 1992.
- [14] J. T. Oden and J. N. Reddy, *Variational Method in Theoretical Mechanics*, Berlin: Springer-Verlag, 1976.
- [15] R. M. Jones, *Mechanics of Composite Materials (second edition)*, CRC Press, 1998.
- [16] V. Yıldırım, "Governing Equations of Initially Twisted Elastic Space Rods Made of Laminated Composite Materials", *International Journal of Engineering Science*, vol. 37, no. 8, pp. 1007-1035, 1999.
- [17] A. Yousefi and A. Rastgoo, "Free Vibration of Functionally Graded Spatial Curved Beams", *Composite Structures*, vol. 93, pp. 3048-3056, 2011.
- [18] M. İnan, *General Theory of Elastic Beams* (in Turkish), İstanbul: Berksoy Printing House, 1966.
- [19] N. Eratlı, M. Yılmaz, K. Darılmaz, M. H. Omurtag, "Dynamic Analysis of Helicoidal bars with non-circular cross-sections via mixed FEM", *Structural Engineering & Mechanics*, vol. 57, no. 2, pp. 221-238, 2016.